ACS APPLIED MATERIALS & INTERFACES

Research Article

www.acsami.org

In Situ STM Investigation of Two-Dimensional Chiral Assemblies through Schiff-Base Condensation at a Liquid/Solid Interface

Fang-Yun Hu,[†,‡,▽] Xue-Mei Zhang,[†,▽] Xiao-Chen Wang,[§] Shuai Wang,[†] Hai-Qiao Wang,[*,§] Wu-Biao Duan,[*,‡] Qing-Dao Zeng,[*,†] and Chen Wang[*,†]

[†]National Center for Nanoscience and Technology (NCNST), Beijing 100190, People's Republic of China

[‡]Department of Chemistry, School of Science, Beijing Jiaotong University, Beijing 100044, People's Republic of China

[§]State Key Laboratory of Organic−Inorganic Composites, College of Materials Science and Engineering, Beijing University of Chemical Technology, Beijing 100029, People's Republic of China

Supporting Information

ABSTRACT: Nanoscaled two-dimensional (2D) chiral architectures are increasingly receiving scientific interest, because of their potential applications in many domains. In this paper, we present a new method for constructing 2D chiral architectures on surface. Based on in situ Schiff-base reaction of achiral dialdehyde with two types of achiral amines at the solid/liquid interface, two chiral species have been directly formed and confirmed by means of a scanning tunneling microscopy (STM) technique. This work introduces a novel strategy to construct 2D surface chirality, which might be applied in fabricating functional films and nanoelectronic devices.

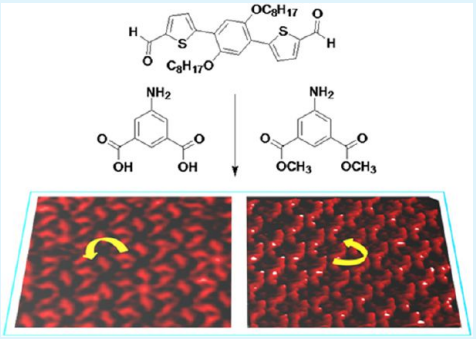

KEYWORDS: *chirality, self-assembly, STM, nanoflower, Schiff-base reaction, two-dimensional*

INTRODUCTION

During the past few years, surface chirality, which is a special type of self-assembly on a solid surface, has gained significant attention, because of its vital relationship with enantioselective catalysis, chiral molecular recognition, and potentially in chiral bioseparation, etc.[1−7] In nature, chiral interfaces are ubiquitous and many materials are intrinsically chiral or possess some chiral crystalline surfaces.[8]

In general, surface chirality can be expressed at two different levels: point chirality and organizational chirality.[9] Most chiral molecules can form a chiral adsorbate on the surface.[10] In recent years, the self-assembly of achiral molecules at crystal surfaces has been expanded enormously, and two-dimensional (2D) chiral structures on solid surface can also be obtained by adsorption of pro-chiral molecules, or even achiral molecules onto the achiral surface (i.e., Au(111), Cu(100), and highly oriented pyrolytic graphite (HOPG)).[7,11−18] Generally, the components with alkyl chains are chosen to build up the chiral assemblies on HOPG, where the flexible alkyl chains play an important role in the formation of chiral patterns.[19−21] One of the well-reported examples is the generation of 2D chiral networks by alkoxylated dehydrobenzo-[12]-annulene (DBA) derivatives at the liquid/solid interface, and the chirality in the hexagonal pores of DBA network results from the relative alignment of the four interdigitated alkyl chains in each pair of DBA molecules.[22] Recently, Liu et al. have successfully achieved the nanoscaled flower-like chiral structure just via the trinary components induced self-assembly on the HOPG surface.[23] These reports focus mainly on the chiral fabrication by physical methods and direct assembly of achiral monocomponents or multicomponents through noncovalent interactions.

Herein, we try to utilize the in situ chemical reactions as a new method for constructing 2D chiral architectures on the HOPG surface. Previous work has shown that chemical reactions (such as photoisomerization, photopolymerization, and condensation reactions) at the interface can be used as an important way of constructing 2D supramolecular self-assembled structures.[24−35] Regulated by the photoisomerization at the solid/liquid interface, a novel 2D triangular molecular network can be transformed from a type of kagomé structure.[36] More recently, utilizing the networks of 1,3,5-tris(10-carboxydecyloxy) benzene (TCDB) as a special molecular template, we have successfully observed the supramolecular coordination of zinc(II) phthalocyanine (Zn-*Pc*) with 1,3-di(4-pyridyl)propane (dipy-pra) in the nano-template, which shows an amazing "odd-even" alternating organization on the HOPG surface.[37] Also, another published work of ours revealed that the reaction of aldehyde with amine on the surface can also be probed by scanning tunneling microscopy (STM), and the assemblies formed by the in situ

Received: September 18, 2012
Accepted: February 4, 2013
Published: February 4, 2013

   dx.doi.org/10.1021/am303236w | *ACS Appl. Mater. Interfaces* 2013, 5, 1583−1587

condensation reaction of aldehyde with amine on the HOPG surface were similar to those formed via the noncovalent physical adsorption of imine, which was synthesized through the ex situ Schiff-base reaction in solution phase.[38]

In this contribution, an achiral dialdehyde derivative and two types of achiral amines are chosen as the active building blocks to construct 2D chiral nanostructures, and such Schiff-base condensation reactions are confirmed by STM at heptanoic acid/HOPG interface.

EXPERIMENTAL SECTION

The dialdehyde derivative, 5,5′-(2,5-bis(octyloxy)-1,4-phenylene) bis-(thiophene-2-carbaldehyde) (PT2, see Figure 1a) was synthesized

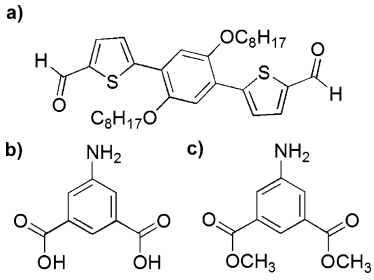

Figure 1. Chemical structures of (a) PT2, (b) 5A-acid, and (c) 5A-ate.

according to the previous report.[39] 5-aminoisophthalic acid (5A-acid, see Figure 1b), dimethyl 5-aminoisophthalate (5A-ate, see Figure 1c), and heptanoic acid were purchased from TCI Company, and used without further purification. All of the studied samples were solved by heptanoic acid, and the concentration of all solutions for STM investigation was less than 1 mM. First, a droplet of solution containing PT2 (0.2 μL) was cast onto a freshly cleaved HOPG (grade ZYB, Advanced Ceramics, Inc., Cleveland, OH, USA). After 20 min, the self-assembled structure was measured by the STM technique. Subsequently, the 5A-acid or 5A-ate solution (0.4 μL) was added to this HOPG surface. Then, the samples were kept at room temperature for approximately one day. After that, the reacted samples were again investigated by STM at the liquid/solid interface. One thing we should mention is that we added some heptanoic acid onto the reacted samples when doing STM investigation, in order to maintain the liquid/solid interface.

The STM measurements were performed under ambient conditions. All STM images presented were acquired on a Nano IIIa scanning probe microscope system (Bruker, USA) operating in constant current mode with mechanically cut Pt/Ir (80/20) tips. The STM images provided are raw data without any treatment except for the flattening procession. The drift is calibrated using the underlying graphite lattice as a reference. The molecular models are built with a HyperChem (6.0) software package.

RESULTS AND DISCUSSION

2D Assembled Structure of the PT2 Molecule at the Heptanoic Acid/HOPG Interface. In this work, with two unsymmetrical aldehyde groups and a pair of alkyl chains, an achiral dialdehyde derivative (PT2) was chosen as an active reagent. Surprisingly, the achiral PT2 molecule displays an amazing chiral assembly on the HOPG surface. As shown in Figure 2b, separated by two domains (A and A′) with a separated angle of $\gamma = 120°$, this angle follows the typical 3-fold structure of the HOPG surface, which implies the existence of chiral structure. With a measured length of 1.0 ± 0.1 nm, the bright sticklike parts can be ascribed to be the conjugated skeleton of the PT2 molecule. Carefully viewing of the molecular models in Figure 2c reveals that the stable structure

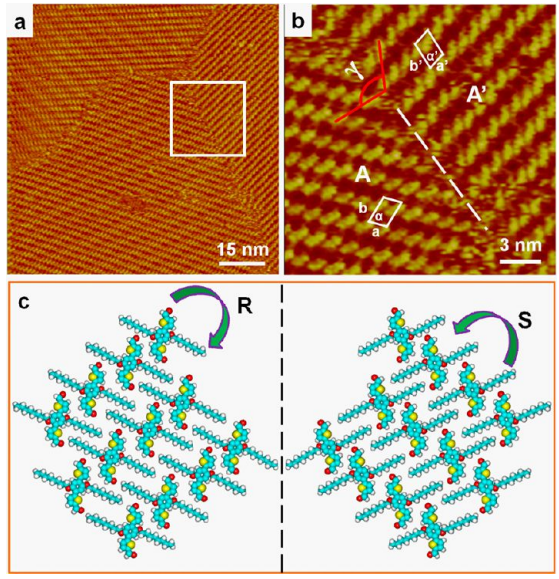

Figure 2. (a) Typical large-scale STM image of the PT2 monolayer at the heptanoic acid/HOPG interface. (b) High-resolution STM image for the white frame area in panel (a). Tunneling parameters: I_{set} = 399.9 pA, V_{bias} = 581.7 mV. (c) Separate molecular model for the arrangement of PT2 in domain A and A′ in panel (b) (legend: cyan (carbon, C), gray (hydrogen, H), red (oxygen, O), and yellow (sulfur, S).

depends on the intermolecular hydrogen bonds as well as the van der Waals interactions. More importantly, because of the flexible property of the alkyl chains, the PT2 molecules in these two domains exhibit different directions. In domain A, the alkyl chains show a clockwise direction while they present a counterclockwise orientation in domain A′, which results in the perfect generation of R- and S- chirality on the surface, separately. On the basis of the symmetry observations and intermolecular distance, two unit cells are superimposed in Figure 2b, with $a = a' = 1.4 \pm 0.1$ nm, $b = b' = 2.2 \pm 0.1$ nm. and $\alpha = \alpha' = 68° \pm 1°$.

In Situ Condensation Reaction of PT2 with 5A-acid at the Heptanoic Acid/HOPG Interface. As described in Scheme 1, when undergoing a typical Schiff-base condensation reaction, a PT2 molecule and two 5A-acid molecules will lose two water molecules and the 5A-acid diimine derivative can be produced.

After some solution containing 5A-acid was applied into the already formed lamellar structures on HOPG, significant change for the assembled structures of PT2 can be clearly viewed. As observed in Figure 3b, the chiral lamella has been replaced by a flower-like architecture. In addition, two types of petals with opposite orientation appeared in two islands (noted as A_1 and A_1'). The formed nanoflowers are also different from the organization of 5-aminoisophthalic acid (Figure 3a),[38] demonstrating that a new compound has been synthesized by the in situ condensation reaction at the liquid/solid interface. According to the reaction equation (see Scheme 1), the new compound should be contributed to the 5A-acid diimine molecule. Careful inspection of the high-resolution images of these two domains (Figures 3c and 3d) reveals that the individual molecule can be clearly divided into three parts (drawn in a three-colored scheme model). With a measured length of 1.0 ± 0.1 nm, the bright lines (drawn in yellow) in both domains correspond to the backbone of the PT2

Scheme 1. Schematic Presentation for the Condensation Reaction of PT2 with 5A-acid and 5A-ate, Respectively

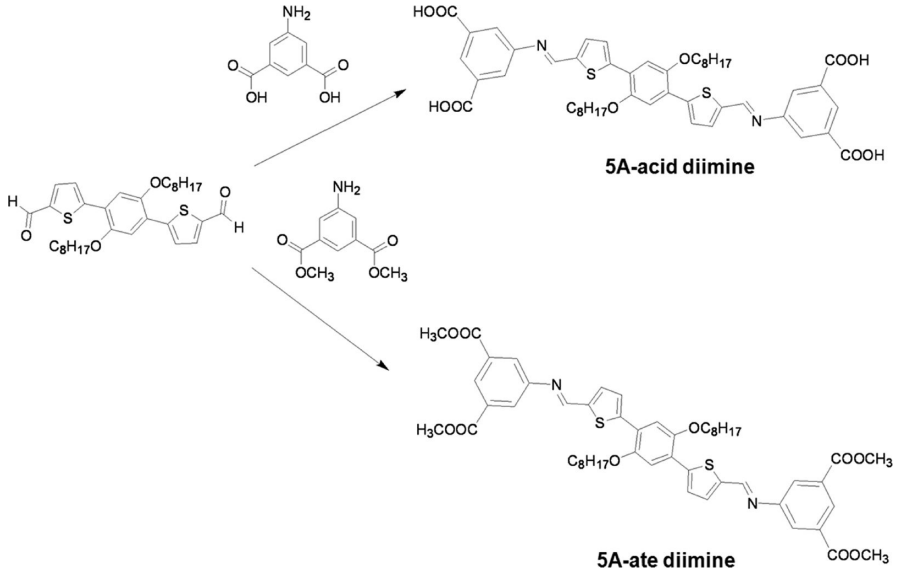

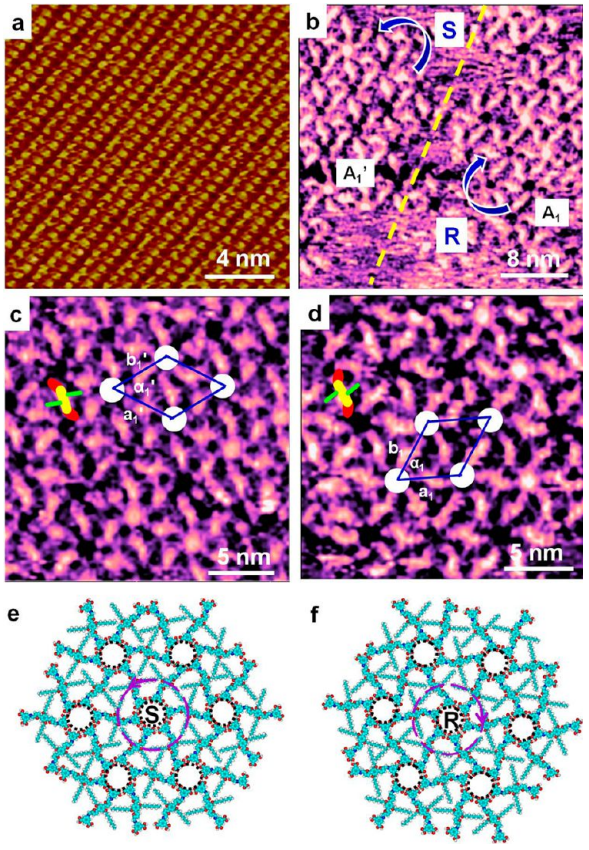

Figure 3. High-resolution STM images for (a) the achiral nano structure of 5A-acid and (b) the chiral flower-like structure of 5A-acid diimine. Also shown are the submolecular assembled structures for (c) domain A_1' and (d) A_1. Panels (e) and (f) show three-color chiral scheme models corresponding to the molecular models for the adlayers shown in panels (c) and (d), respectively, that was deposited on these STM images. (Tunneling parameters: I_{set} = 390.6 pA, V_{bias} = 649.7 mV. Legend: cyan (carbon, C), gray (hydrogen, H), red (oxygen, O), yellow (sulfur, S), blue (nitrogen, N)).

molecules. In each domain, every 5A-acid diimine molecule connects with two neighboring 5A-acid diimine molecules by hydrogen bonds between the carboxyl groups. And six 5A-acid diimine molecules assembled into a nanoflower structure through six pairs of COOH···HOOC hydrogen bonds. Therefore, every 5A-acid diimine molecule can be shared by two adjacent architectures, and every flower is surrounded by six flowers, to form an extended nanoflower architecture. Besides, in each domain, there appears to be a nanocavity in the center of each flower, with a radius of $R = 1.3 \pm 0.1$ nm. In addition, irregular bright spots can be viewed in some cavities, which should be ascribed to the adsorption of the solvent molecules or the 5A-acid molecules. Obviously, the orientations for domains A_1 and A_1' are opposite to each other. For domain A_1 (Figure 3d), the 5A-acid diimine molecules orientate in a clockwise direction, presenting the R-configurational assembly, whereas in domain A_1' (Figure 3c), the flowers open in a counterclockwise direction, which displays S-configurational assembly. The observed chiral assembled area shows a unit cell with the folllowing measurement parameters: $a_1 = a_1' = b_1 = b_1' = 4.6 \pm 0.1$ nm, and $\alpha_1 = \alpha_1' = 60 \pm 1°$.

In Situ Condensation Reaction of PT2 with 5A-ate at the Heptanoic Acid/HOPG Interface. Figure 4a presents a typical assembled structure of 5-aminoisophthalate (5A-ate) molecules on the surface. In the submolecular resolved structure, with a size of 0.7 ± 0.1 nm, every spot (indicated by the white ball) corresponds to a 5A-ate molecule. Four 5A-ate molecules connect into a tetramer through the weak intermolecular NH···HN hydrogen bonds to form a fan-shaped structure.

Upon the addition of 5A-ate into the assembled structure of the PT2 molecules, another chiral lamellar structure replaces the former monolayer (see Figure 4b); this transformation should be attributed to the condensation of one PT2 molecule with two 5A-ate molecules. Similar to the reaction of PT2 with 5A-acid, the 5A-ate molecules can also react with PT2 molecules by Schiff-base reaction (see Scheme 1), resulting the formation of the 5A-ate diimine compound. In other words, the new lamella is formed by the 5A-ate diimine molecules.

The individual molecule can be well-resolved from the two high-resolution STM images (see Figures 4c and 4d). The 5A-ate diimine molecule clearly shows a three-color worm-shaped structure consisting of a head, a body, and a tail, as well as two

dx.doi.org/10.1021/am303236w | ACS Appl. Mater. Interfaces 2013, 5, 1583−1587

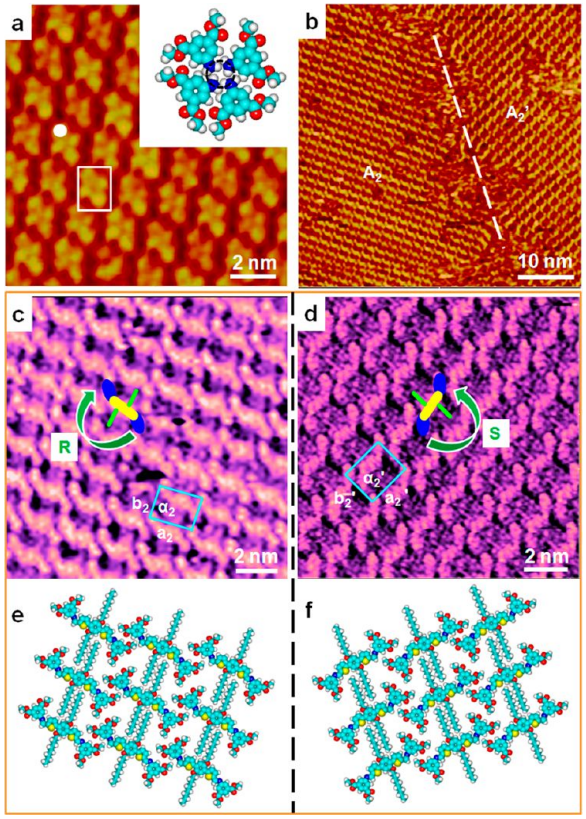

Figure 4. (a) Lamellar structure of 5A-ate at the heptanoic acid/HOPG interface (I_{set} = 360.1 pA, V_{bias} = 652.7 mV) (inset shows a tentative molecular model for the area drawn in the white frame). (b) Large-scale STM image of a monolayer formed by the 5A-ate diimine molecule. I_{set} = 387.6 pA, V_{bias} = 607.9 mV. Also shown are submolecular structures for (c) domain A_2 and (d) A_2' (the unit cells are superimposed onto these two images). (e and f) Suggested molecular models for the assemblies in domain A_2 and A_2', respectively. (Legend: cyan (carbon, C), gray (hydrogen, H), red (oxygen, O), yellow (sulfur, S), blue (nitrogen, N).)

wings. The length of the headlike and tail-like portion (drawn in blue) is 0.7 ± 0.1 nm, which is well in agreement with the length of the 5A-ate molecule. Also, the measured length of the center part (drawn in yellow) is 1.0 ± 0.1 nm, corresponding to the body of the PT2 molecule. Besides, the distance between two neighboring lamellae is measured to be 1.0 ± 0.1 nm, which is consistent with the length of alkyl chain (drawn in green). By the two formed covalent C=N bonds, the body connects with the head and tail to compose a worm-like architecture. From the molecular models in Figures 4e and 4f, the alkyl chains of the 5A-ate diimine interdigitate with two neighbors through the weak van der Waals interactions between alkyl chains. As a result, four neighboring 5A-ate diimine molecules in both domains fabricate a rectangular network.

Similar to those of the chiral assemblies of 5A-acid diimine molecule, the structures of 5A-ate dimine also display the surface chirality, one for R-configuration and another for S-configuration with the same characteristic parameters ($a_2 = a_2' = 1.9 \pm 0.1$ nm, $b_2 = b_2' = 1.7 \pm 0.1$ nm, $\alpha_2 = \alpha_2' = 90° \pm 2°$). [R denotes a clockwise orientation, whereas S denotes a counterclockwise orientation.]

Based on the above-mentioned description and discussions, we can conclude that the condensation reaction between dialdehyde and amine indeed happens, which is also demonstrated by the same STM results of these two diimine molecules synthesized by ex situ method in the solution phase (see the Supporting Information). Meanwhile, we believe that it is highly possible that this type of chemical reaction occurred at the solid/liquid interface. Comparing these two supramolecular chiral architectures, it is not hard to illustrate that the self-assembled behavior of the target molecules are mainly dominated by two types of hydrogen bonding interactions. On the surface, it should be noted that the acid solvent is beneficial to such Schiff-base condensation, which is similar to those reactions that occurred in solution.[40] Besides, we should note that the ratio of amine and dialdehyde is more than 2:1, because some amine derivatives in heptanoic acid solution will be transformed to their ionic salts, which cannot react well with the dialdehyde compounds.

CONCLUSIONS

Herein, we present two types of two-dimensional (2D) chiral assemblies by an in situ Schiff-base condensation reaction of achiral dialdehyde (PT2) with two achiral aromatic amine derivatives at the heptanoic acid/HOPG interface. The achiral PT2 molecules can form chiral lamellar adlayers. Upon the addition of achiral 5-aminoisophthalic acid (5A-acid) or dimethyl 5-aminoisophthalate (5A-ate), the chiral lamellar structure can be transformed to the chiral nanoflower or nanoworm architectures, respectively. It is found that the transformations of structures result from the occurrence of the condensation reaction on the surface at room temperature. Also, the intermolecular hydrogen bonds play an important role in the construction of these two amazing chiral structures. This research provides a new method to construct 2D chiral self-assembled systems, which can be potentially applied to the fabrication of functional films and nanodevices.

ASSOCIATED CONTENT

Supporting Information

The detailed synthesis procedures, ^{1}H NMR and mass spectra of the target diimine molecules, and STM images for the assembly structure of the two diimine prepared ex situ. This material is available free of charge via the Internet at http://pubs.acs.org.

AUTHOR INFORMATION

Corresponding Author

*E-mail addresses: zengqd@nanoctr.cn (Q.-D.Z.), wangch@nanoctr.cn (C.W.), wbduan@bjtu.edu.cn (W.-B.D.), wanghaiqiao@mail.buct.edu.cn (H.-Q.W.).

Author Contributions

$^{\nabla}$F.-Y.H. and X.-M.Z. contributed equally to this work.

Notes

The authors declare no competing financial interest.

ACKNOWLEDGMENTS

This work was supported by the National Basic Research Program of China (Nos. 2011CB932303 and 2013CB934200). Financial supports from National Natural Science Foundation of China (Nos. 21073048, 51173031, and 91127043) are also gratefully acknowledged.

REFERENCES

(1) Kuhnle, A.; Linderoth, T. R.; Hammer, B.; Besenbacher, F. *Nature* **2002**, *415*, 891−893.
(2) Fasel, R.; Parschau, M.; Ernst, K. H. *Nature* **2006**, *439*, 449−452.
(3) Elemans, J. A. A. W.; De Cat, I.; Xu, H.; De Feyter, S. *Chem. Soc. Rev.* **2009**, *38*, 722−736.
(4) De Cat, I.; Gobbo, C.; Van Averbeke, B.; Lazzaroni, R.; De Feyter, S.; Van Esch, J. *J. Am. Chem. Soc.* **2011**, *133*, 20942−20950.
(5) Weissbuch, I.; Leiserowitz, L.; Lahav, M. *Curr. Opin. Colloid Interface Sci.* **2008**, *13*, 12−22.
(6) Zhang, Y. Q.; Chen, P. L.; Ma, Y. P.; He, S. G.; Liu, M. H. *ACS Appl. Mater. Interfaces* **2009**, *1*, 2036−2043.
(7) Raval, R. *Chem. Soc. Rev.* **2009**, *38*, 707−721.
(8) Hazen, R. M.; Sholl, D. S. *Nat. Mater.* **2003**, *2*, 367−374.
(9) Sun, K.; Shao, T. N.; Xie, J. L.; Lan, M.; Yuan, H. K.; Xiong, Z. H.; Wang, J. Z.; Liu, Y.; Xue, Q. K. *Small* **2012**, *8*, 2078−2082.
(10) Ernst, K. H. *Top. Curr. Chem.* **2006**, *265*, 209−252.
(11) De Feyter, S.; De Schryver, F. C. *J. Chem. Phys. B* **2005**, *109*, 4290−4302.
(12) Shen, Y. T.; Deng, K.; Zeng, Q. D.; Wang, C. *Small* **2010**, *6*, 76−80.
(13) Li, C. J.; Zeng, Q. D.; Wu, P.; Xu, S. L.; Wang, C.; Qiao, Y. H.; Wan, L. J.; Bai, C. L. *J. Phys. Chem. B* **2002**, *106*, 13262−13267.
(14) Gutzler, R.; Ivasenko, O.; Fu, C. Y.; Brusso, J. L.; Rosei, F.; Perepichka, D. F. *Chem. Commun.* **2011**, *47*, 9453−9455.
(15) Kim, B. I.; Kim, S. *Langmuir* **2012**, *28*, 8010−8016.
(16) Barlow, S. M.; Louafi, S.; Roux, D. L.; Williams, J.; Muryn, C.; Haq, S.; Raval, R. *Langmuir* **2004**, *20*, 7171−7176.
(17) Silly, F.; Shaw, A. Q.; Castelle, M. R.; Briggs, G. A. D. *Chem. Commun.* **2008**, 1907−1909.
(18) Yang, B.; Wang, Y. L.; Cun, H. Y.; Du, S. X.; Xu, M. C.; Wang, Y.; Ernst, K. H.; Gao, H. J. *J. Am. Chem. Soc.* **2010**, *132*, 10440−10444.
(19) Guo, Z. X.; De Cat, I.; Van Averbeke, B.; Lin, J. B.; Wang, G. J.; Xu, H.; Lazzaroni, R.; Beljonne, D.; Meijer, E. W.; Schenning, A. P. H. J.; De Feyter, S. *J. Am. Chem. Soc.* **2011**, *133*, 17764−17771.
(20) De Cat, I.; Guo, Z. X.; George, S. J.; Meijer, E. W.; Schenning, A. P. H. J.; De Feyter, S. *J. Am. Chem. Soc.* **2012**, *134*, 3171−3177.
(21) Chen, Q.; Chen, T.; Wang, D.; Liu, H. B.; Li, Y. L.; Wan, L. J. *Proc. Natl. Acad. Sci. U.S.A.* **2010**, *107*, 2769−2774.
(22) Tahara, K.; Yamaga, H.; Ghijsens, E.; Inukai, K.; Adisoejoso, J.; Blunt, M. O.; De Feyter, S.; Tobe, Y. *Nat. Chem.* **2011**, *3*, 714−719.
(23) Liu, J.; Chen, T.; Deng, X.; Wang, D.; Pei, J.; Wan, L. J. *J. Am. Chem. Soc.* **2011**, *133*, 21010−21015.
(24) Furukawa, S.; Tahara, K.; De Schryver, F. C.; Auweraer, M. V.; Tobe, Y.; De Feyter, S. *Angew. Chem., Int. Ed.* **2007**, *46*, 2831−2834.
(25) Saiz Poseu, J.; Faraudo, J.; Figueras, A.; Alibes, R.; Busque, F.; Ruiz Molina, D. *Chem.—Eur. J.* **2012**, *18*, 3056−3063.
(26) Zhang, X. M.; Xu, S. D.; Li, M.; Shen, Y. T.; Wei, Z. Q.; Wang, S.; Zeng, Q. D.; Wang, C. *J. Phys. Chem. C* **2012**, *116*, 8950−8955.
(27) Mali, K. S.; Adisoejoso, J.; Ghijsens, E.; De Cat, I.; De Feyter, S. *Acc. Chem. Res.* **2012**, *45*, 1309−1320.
(28) Tanoue, R.; Higuchi, R.; Enoki, N.; Miyasato, Y.; Uemura, S.; Kimizuka, N.; Stieg, A. Z.; Gimzewski, J. K.; Kunitake, M. *ACS Nano* **2011**, *5*, 3923−3929.
(29) Dienstmaier, J. F.; Gigler, A. M.; Goetz, A. J.; Knochel, P.; Bein, T.; Lyapin, A.; Reichlmaier, S.; Heckl, W. J.; Lackinger, M. *ACS Nano* **2011**, *5*, 9737−9745.
(30) Weigelt, S.; Busse, C.; Bombis, C.; Knudsen, M. M.; Gothelf, K. V.; Strunskus, T.; Woll, C.; Dahlbom, M.; Hammer, B.; Lægsgaard, E.; Besenbacher, F.; Linderoth, T. R. *Angew. Chem., Int. Ed.* **2007**, *46*, 9227−9230.
(31) Weigelt, S.; Busse, C.; Bombis, C.; Knudsen, M. M.; Gothelf, K. V.; Lægsgaard, E.; Besenbacher, F.; Linderoth, T. R. *Angew. Chem., Int. Ed.* **2008**, *47*, 4406−4410.
(32) Miura, A.; De Feyter, S.; Abdel-Mottaleb, M. M. S.; Gesquière, A.; Grim, P. C. M.; Moessner, G.; Siefert, M.; Klapper, M.; Müllen, K.; De Schryver, F. C. *Langmuir* **2003**, *19*, 6474−6482.
(33) Shen, Y. T.; Deng, K.; Zhang, X. M.; Feng, W.; Zeng, Q. D.; Wang, C.; Gong, J. R. *Nano Lett.* **2011**, *11*, 3245−3250.
(34) Kikkawa, Y.; Omori, K.; Takahashi, M.; Kanesato, M.; Hiratani, K. *Org. Biomol. Chem.* **2012**, *10*, 8087−8094.
(35) Tanoue, R.; Higuchi, R.; Ikebe, K.; Uemura, S.; Kimizuka, N.; Stieg, A. Z.; Gimzewski, J. K.; Kunitake, M. *Langmuir* **2012**, *28*, 13844−13851.
(36) Zhang, X. M.; Wang, S.; Shen, Y. T.; Guo, Y. Y.; Zeng, Q. D.; Wang, C. *Nanoscale* **2012**, *4*, 5039−5042.
(37) Zhang, X. M.; Shen, Y. T.; Wang, S.; Guo, Y. Y.; Deng, K.; Wang, C.; Zeng, Q. D. *Sci. Rep.* **2012**, *2*, 742.
(38) Li, Y. B.; Wan, J. H.; Deng, K.; Han, X. N.; Lei, S. B.; Yang, Y. L.; Zheng, Q. Y.; Zeng, Q. D.; Wang, C. *J. Phys. Chem. C* **2011**, *115*, 6540−6544.
(39) Promarak, V.; Ruchirawat, S. *Tetrahedron* **2007**, *63*, 1602−1609.
(40) Sprung, M. A. *Chem. Rev.* **1940**, *26*, 297−338.